

## Rovibrational Energy Transfer in Methane Excited to $2\nu_3$ in $\text{CH}_4\text{-N}_2$ Mixtures from Double-Resonance Measurements

F. Menard-Bourcin, C. Boursier, L. Doyennette, and J. Menard\*

Laboratoire de Physique Moléculaire et Applications, CNRS, Université Pierre et Marie Curie, Tour 13 - Bte 76, 4, place Jussieu, 75252 Paris Cedex 05, France

Received: May 4, 2001; In Final Form: October 12, 2001

The rovibrational energy transfer processes occurring in methane upon inelastic  $\text{CH}_4\text{-N}_2$  collisions have been investigated by using time-resolved double-resonance (DR) measurements. The  $\text{CH}_4$  molecules were excited at about  $1.66\ \mu\text{m}$  into selected rotational levels of the  $2\nu_3(\text{F}_2)$  state by an optical parametric oscillator pumped by a Nd:YAG laser. The low power beam of a tunable diode laser emitting around  $3.4\ \mu\text{m}$  was used to probe the following transitions:  $(\nu_3 + \nu_4) \leftarrow \nu_4$ ,  $2\nu_3 \leftarrow \nu_3$ ,  $(\nu_3 + 2\nu_4) \leftarrow 2\nu_4$ , and  $3\nu_3 \leftarrow 2\nu_3$  transitions. Measurements were performed in  $\text{CH}_4\text{-N}_2$  gas mixtures with various molar fractions of methane. Rate constants were deduced from the time evolution of the transient populations of the probed levels.  $\text{N}_2$  has been found to be an efficient collision partner to deplete the laser-excited level through rotational energy transfer, with a rate constant of  $(13.0 \pm 1.5)\ \mu\text{s}^{-1}\ \text{Torr}^{-1}$  and through intermode transfer to equilibrate the populations among the states of the tetradecad, with a rate constant of  $(2.0 \pm 0.6)\ \mu\text{s}^{-1}\ \text{Torr}^{-1}$ . These measurements have allowed us to determine the part played in the vibrational relaxation by intermode transfer processes, which occur between the strongly interacting states of the polyads upon  $\text{CH}_4\text{-CH}_4$  as well as  $\text{CH}_4\text{-N}_2$  collisions, and by near-resonant V–V energy transfer processes coupling the tetradecad to lower polyads, which occur only upon  $\text{CH}_4\text{-CH}_4$  collisions.

### Introduction

In a previous work,<sup>1</sup> we have presented a preliminary study of the vibrational relaxation of methane after its excitation into the  $2\nu_3(\text{F}_2)$  state by a laser radiation around  $6000\ \text{cm}^{-1}$ . From the observed laser-induced fluorescence, we obtained a first understanding of the main processes implied in the return to equilibrium of this gas.

Recently,<sup>2</sup> we have shown that the transfers of rotational and vibrational energy that occur in  $\text{CH}_4$  under the effect of collisions could be thoroughly studied with the time-resolved IR–IR double-resonance technique. Indeed, this technique has been largely improved during the past few years owing to the recent progress in tunable laser sources in the infrared. Optical parametric oscillators (OPO) are very good sources to pump molecules in selected vibration–rotation levels because they can now produce laser pulses with a very small spectral width, as narrow as  $0.02\ \text{cm}^{-1}$  in our experiments. On the other hand, single mode lead-salt laser diodes, with a spectral width of  $0.002\ \text{cm}^{-1}$  are very convenient sources to continuously probe a selected transition between two rovibrational levels.

From the double-resonance measurements reported in ref 2, many data on the relaxation of methane were obtained: determination of the rate constants for rotational energy transfer, and for vibrational energy transfer, in particular intermode transfers (between bending and stretching modes) and near-resonant V–V energy transfers. But these measurements were performed in neat methane. In view of future atmospheric applications in which the methane could be used as a probe of its environment, it was also necessary to investigate the energy transfers that occur in  $\text{CH}_4$  under the effect of collisions with the main atmospheric constituents.

The aim of the present paper is to give the results obtained in  $\text{CH}_4\text{-N}_2$  mixtures and to show how they improve our understanding of the relaxation pathway as compared to the neat methane analysis. Besides, new results were obtained concerning the transfer of energy between different symmetry species and, moreover, the detection of a new unassigned transition between a bending state of the pentad and a combination state of the tetradecad corroborates the interpretation of the results and demonstrates the interest of the technique to assign new lines.

### Experimental Setup

Details about the double-resonance experimental technique used to study the collisional relaxation of vibrationally excited methane molecules can be found in ref 2. We briefly recall here the main features. The 7 ns output pulse of the OPO pumped by a single mode Nd:YAG laser (Continuum) is used to excite  $\text{CH}_4$  via selected rovibrational transitions of the  $2\nu_3(\text{F}_2) \leftarrow 0$  band near  $6000\ \text{cm}^{-1}$ . Under the effect of collisions in molecular mixtures, the rovibrationally excited methane molecules return to equilibrium. The low power infrared beam provided by a CW single mode lead-salt diode laser (Laser Photonics), tunable in the  $2935\text{--}2983\ \text{cm}^{-1}$  range, is used to probe the transient populations of selected levels in methane via asymmetric stretch transitions. It is collinearly propagated and overlaps with the pump pulse through the double resonance cell by means of a dichroic beam splitter, coated to provide high reflectivity around  $3000\ \text{cm}^{-1}$  while transmitting  $\sim 85\%$  of the  $6000\ \text{cm}^{-1}$  pulse. The sample cell is made from a Pyrex tube 60 cm long with an internal diameter of 38 mm.  $\text{CaF}_2$  windows are held on each end. The residual pulsed beam at the exit of the sample cell is ruled out by means of a same dichroic beam splitter reflecting only the probe beam. Then, the probe beam is focused onto a liquid nitrogen cooled InSb detector (SAT). The detector/

\* To whom correspondence should be addressed. Fax: 33 (0)1 44 27 70 33. E-mail: menard@ccr.jussieu.fr.

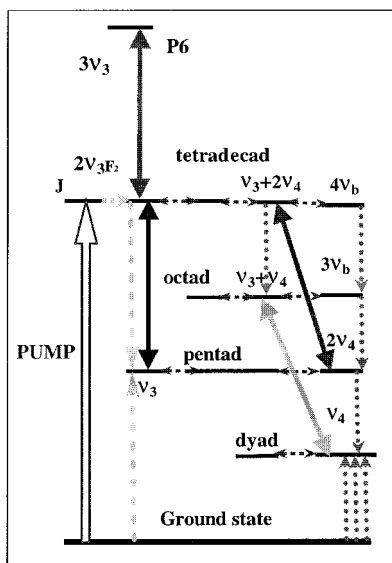


**Figure 1.** Simplified diagram of the vibrational energy levels of methane showing the lowest polyads of interacting states. The arrows, in full lines, show the transitions probed in the present experiments, and, in dotted lines, collisional intermode transfers between states of each polyad and near-resonant V–V transfers coupling the polyads.

amplifier combination has a rise time lower than 200 ns. The signal from the InSb detector is sampled, averaged, and stored on a Tektronix DSA 601 digital signal analyzer before being transmitted to a computer for further analysis. To eliminate the scattered radiation coming from the pump pulse and the electrical disturbance from the Pockels cell in the Nd:YAG laser, a reference signal, recorded in the same condition except for the probe beam that is frequency shifted, is subtracted from each DR signal before analysis.

## Results

The spectroscopic peculiarities of the CH<sub>4</sub> spherical-top molecule have been summarized in our previous papers<sup>1,2</sup> and will not be repeated here. Let us only recall that all the vibrational states of methane are gathered in polyads of interacting states that are spaced by about 1500 cm<sup>-1</sup> in energy. As schematically shown in Figure 1, the lowest polyads considered in this work are successively a dyad, a pentad, an octad, a tetradecad involving the 2ν<sub>3</sub> laser-excited state, and a higher polyad called P<sub>6</sub> involving the 3ν<sub>3</sub> state. To investigate the relaxation path in neat methane,<sup>2</sup> three types of transitions have been probed: 3ν<sub>3</sub> ← 2ν<sub>3</sub>(F<sub>2</sub>), 2ν<sub>3</sub>(F<sub>2</sub>) ← ν<sub>3</sub>, and various octad ← dyad transitions. After revisiting the double-resonance (DR) signals observed by scanning the frequency of the diode laser emission, we have found a new kind of signal at 2970.50 cm<sup>-1</sup>. It may be assigned to the (ν<sub>3</sub> + 2ν<sub>4</sub>), J = 2, A<sub>1</sub>, 11 ← 2ν<sub>4</sub>, J = 3, A<sub>2</sub>, 1 transition<sup>3,4</sup> from the data provided to us by O. Robert and J.-P. Champion from their spectroscopic analysis of the tetradecad. So, we have now at our disposal four types of probe transitions as indicated in Figure 1.

**Rotational Relaxation.** The rotational relaxation of the excited level is directly observed by choosing the diode frequency in such a way that the lower level of the probed transition is the excited level. Two such typical DR signals are shown in Figure 2. The pump laser is tuned to the frequency of the Q<sub>4</sub> line of the 2ν<sub>3</sub>(F<sub>2</sub>) ← 0 band at 6003.89 cm<sup>-1</sup>, which leads to excitation of CH<sub>4</sub> molecules into the 2ν<sub>3</sub>(F<sub>2</sub>) J = 4, A<sub>2</sub>, 43 level. The diode laser is tuned to 2939.79 cm<sup>-1</sup>, which corresponds to a 3ν<sub>3</sub> ← 2ν<sub>3</sub>(F<sub>2</sub>) J = 4, A<sub>2</sub>, 43 transition. The

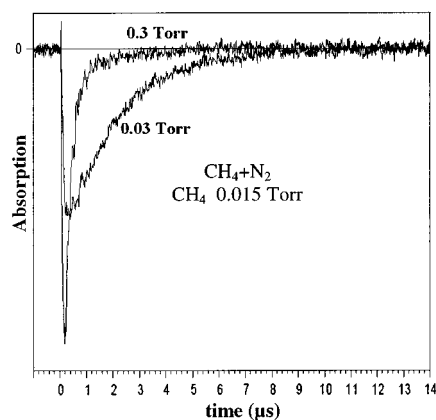


**Figure 2.** DR signals showing the time evolution in population of the laser-excited level. They are obtained by exciting, via the Q<sub>4</sub> line, CH<sub>4</sub> molecules into the 2ν<sub>3</sub>(F<sub>2</sub>) J = 4, A<sub>2</sub>, 43 level, and by probing a 3ν<sub>3</sub> ← 2ν<sub>3</sub>(F<sub>2</sub>) J = 4, A<sub>2</sub>, 43 transition. In both CH<sub>4</sub> + N<sub>2</sub> mixtures, the methane pressure is 15 mTorr, and the total pressure 0.03 and 0.3 Torr, respectively.

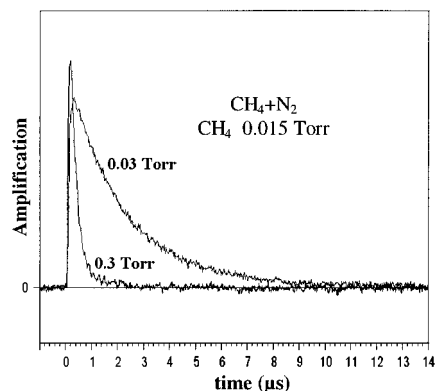


**Figure 3.** DR signals obtained by exciting, via the R<sub>0</sub> line, CH<sub>4</sub> molecules into the 2ν<sub>3</sub>(F<sub>2</sub>) J = 1, A<sub>2</sub>, 18 level, and by probing the 2ν<sub>3</sub>(F<sub>2</sub>), J = 1, A<sub>2</sub>, 18 ← ν<sub>3</sub>, J = 2, A<sub>1</sub>, 4 transition. The gas pressures are the same ones as for the signals of Figure 2.

methane pressure is 15 mTorr with nitrogen pressure being 1 and 19 times the methane pressure. These signals exhibit a quasi instantaneous decay in transmission of the probe beam (in the limit of electronic response), due to the increase in population of the laser-excited level, followed by a rise due to the depletion of this J level by collisional processes of rotational energy transfer. It is clearly seen that the nitrogen molecules are efficient collision partners for rotational relaxation. Such DR signals may be analyzed by fitting the rising part of the curve to a sum of two exponential functions of time. The pressure-dependent rotational relaxation rate is extracted from the fastest exponential that is also the strongest one. In CH<sub>4</sub>–N<sub>2</sub> mixtures involving a same methane partial pressure, the rate varies linearly with the nitrogen pressure, and the rate constant of rotational relaxation corresponding to CH<sub>4</sub> + N<sub>2</sub> collisions is deduced from the slope of this linear variation.

Another type of probe transition has been used to investigate the rotational relaxation. When the rotational level excited by the pump laser is no longer the lower level of the probed transition but the upper level, the DR signals exhibit an initial amplification followed by a fast decay. For instance, in Figure 3 the pump laser is tuned to the R<sub>0</sub> line at 6015.66 cm<sup>-1</sup>, which excites methane into the 2ν<sub>3</sub>(F<sub>2</sub>), J = 1, A<sub>2</sub>, 18 level while this level is monitored via the 2ν<sub>3</sub>(F<sub>2</sub>), J = 1, A<sub>2</sub>, 18 ← ν<sub>3</sub>, J = 2, A<sub>1</sub>, 4 transition at 2963.99 cm<sup>-1</sup>. Obviously, these two signals, obtained with the same pressures as the signals of Figure 2,

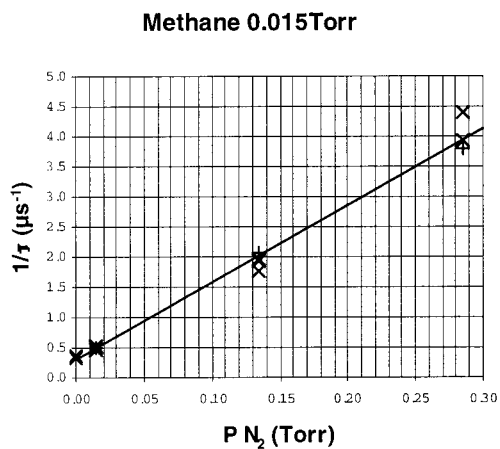


**Figure 4.** Plot of the measured rotational relaxation rates versus nitrogen pressure for  $\text{CH}_4\text{-N}_2$  mixtures with the same methane pressure of 15 mTorr. The data have been obtained by probing the laser excited level via a  $3\nu_3 \leftarrow 2\nu_3$  transition (+) as in Figures 2 and  $2\nu_3 \leftarrow \nu_3$  transitions (x) as in Figure 3: The slope of the straight line is  $12.8 \mu\text{s}^{-1} \text{Torr}^{-1}$ .

have essentially the same time behavior except for the direction of deviation.

Similar DR signals have been obtained with other pump-probe combinations. All these signals can be analyzed by fitting the decaying part of the DR signal to a sum of two exponential functions of time. The pressure-dependent relaxation rates extracted from the fastest exponential are in close agreement with those obtained with the previous DR signals as can be seen in Figure 4 where a typical plot of the measured relaxation rates versus nitrogen pressure is shown for a same methane pressure of 15 mTorr. The data reported in Figure 4 have been obtained for three pump-probe combinations: the pump tuned to  $Q_4$  with the probe tuned to  $2939.79 \text{ cm}^{-1}$  as in Figure 2, the pump tuned to  $R_0$  with the probe tuned to  $2963.99 \text{ cm}^{-1}$  as in Figure 3, and the pump tuned to  $Q_3$  at  $6004.29 \text{ cm}^{-1}$  with the probe tuned to the  $2\nu_3(\text{F}_2)$ ,  $J = 3$ ,  $A_1$ ,  $32 \leftarrow \nu_3$ ,  $J = 4$ ,  $A_2$ , 5 transition at  $2944.69 \text{ cm}^{-1}$ . All these data are well fitted by a straight line the slope of which is  $12.8 \mu\text{s}^{-1} \text{Torr}^{-1}$ .

Various sets of measurements have been made by pumping to various  $J$  levels from  $J = 1$  to  $J = 4$  and by probing either  $3\nu_3 \leftarrow 2\nu_3(\text{F}_2)$  transitions or  $2\nu_3(\text{F}_2) \leftarrow \nu_3$  transitions at methane pressure ranging from 0.002 to 0.2 Torr and methane molar fractions down to 1.75%. For a given molar fraction, the relaxation rate was found to be proportional to the total pressure, and thence a rate constant can be determined for each molar fraction. The mean values obtained by taking into account all the DR signals are plotted in Figure 5 versus the methane molar fraction.

From these results, one can deduce the values for the rotational self-relaxation and for the relaxation upon nitrogen-methane collisions, namely,  $(20.8 \pm 2.5)$  and  $(13.0 \pm 1.5) \mu\text{s}^{-1} \text{Torr}^{-1}$ , respectively.

Now, by probing again  $3\nu_3 \leftarrow 2\nu_3(\text{F}_2)$  or  $2\nu_3(\text{F}_2) \leftarrow \nu_3$  transitions but in which the rotational state of  $2\nu_3(\text{F}_2)$  is not directly laser-excited, it is possible to observe the transfer from one rotational state to another one. Only states of the same symmetry type as that of the laser-excited level are populated, as explained in ref 2, but within this symmetry type the redistribution is very fast. For instance, after excitation into the  $J = 4$ ,  $A_2$ , 43 level the delay time to reach maximum population in the  $J = 2$ ,  $A_1$ , 29 is shorter than  $0.6 \mu\text{s}$  for a 0.2 Torr mixture with 50% methane molar fraction, and it decreases very rapidly as  $\text{N}_2$  is added. So, it is necessary to take measurements at very

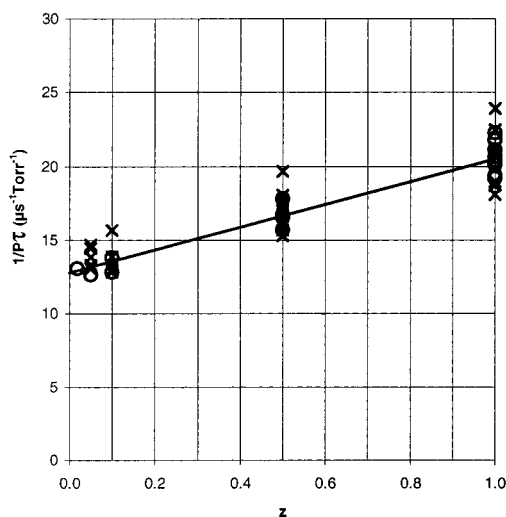


**Figure 5.** Variation, versus the methane molar fraction  $z$ , of the rotational energy transfer rate constants deduced from various sets of measurements performed by pumping  $J$  levels from  $J = 1$  to  $J = 4$  and by probing  $3\nu_3 \leftarrow 2\nu_3(\text{F}_2)$  transitions (O) as well as  $2\nu_3(\text{F}_2) \leftarrow \nu_3$  transitions (x) at methane pressure ranging from 0.002 to 0.2 Torr and methane molar fractions down to 1.75%.

low pressure. Unfortunately, because these rotational redistribution processes are very fast and because the number of implied levels is large, the signals obtained in the required pressure range are rather weak, and it was not possible to measure with enough accuracy the detailed state to state rotational energy transfer processes.

**Vibrational Relaxation.** After an equilibrium has been established in the  $2\nu_3(\text{F}_2)$  vibrationally excited state among the rotational levels belonging to the same symmetry type as that of the laser-excited level, the energy is spread out by vibrational relaxation into the other vibrational states. The induced changes in population can be well visualized with the various probes at our disposal. Typically, three DR signals obtained for a same gas sample with three different probes corresponding to A symmetry species and with the pump laser tuned to the A symmetry component of  $Q_4$  are shown in Figure 6. The methane pressure is 0.6 Torr, and the nitrogen pressure is 34 Torr. A first DR signal (top signal) is obtained by probing the  $2\nu_3(\text{F}_2)$ ,  $J = 1$ ,  $A_2$ ,  $18 \leftarrow \nu_3$ ,  $J = 2$ ,  $A_1$ , 4 transition; the second signal (middle signal) has been assigned to the  $(\nu_3 + 2\nu_4)$ ,  $J = 2$ ,  $A_1$ ,  $11 \leftarrow 2\nu_4$ ,  $J = 3$ ,  $A_2$ , 1 transition, and the bottom signal corresponds to the  $(\nu_3 + \nu_4)$ ,  $J = 5$ ,  $A_2$ ,  $14 \leftarrow \nu_4$ ,  $J = 6$ ,  $A_1$ , 1 dyad-octad transition. On the top signal, one can observe a fast initial rise showing that a fast increase in population occurs in the  $2\nu_3(\text{F}_2)$ ,  $J = 1$   $A_2$  upper level of the transition, due to rotational energy transfer from  $J = 4$  to  $J = 1$ . Then, the amplification decreases as this state is depleted. At the same time, the middle signal increases slightly providing evidence of intermode transfer processes populating the  $(\nu_3 + 2\nu_4)$  vibrational state. After about  $1 \mu\text{s}$ , the top signal and the middle signal exhibit an absorption of the probe beam as a result of an increase of population in the lower levels of the probed transitions,  $\nu_3$  and  $2\nu_4$ , respectively, showing that both bending and stretching states of the pentad are filling up. Considering the time behavior and the position of the minimum in the top and middle signals, which corresponds to the maximum transient population in pentad states, it appears that the stretching and bending levels of the pentad proceed at similar rates. During this period, the bottom signal decreases as the  $\nu_4$  level is filling. While at about  $4 \mu\text{s}$  the population in the pentad states begins to decrease, the bottom signal is still decreasing, which shows

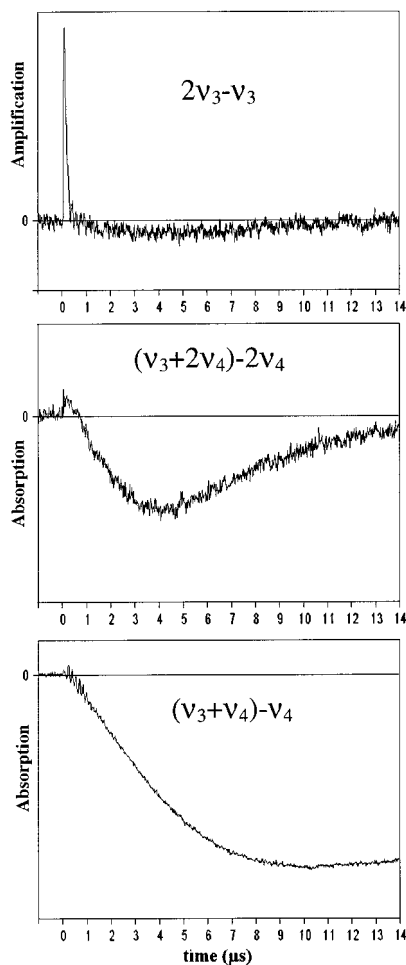


**Figure 6.** DR signals obtained, with 0.6 Torr methane pressure and 34 Torr nitrogen pressure, by pumping  $\text{CH}_4$  molecules with the laser tuned to the A symmetry component of  $Q_4$ , and probing A symmetry species via three different transitions successively a  $2\nu_3 \leftarrow \nu_3$  transition (top signal), a  $(\nu_3 + 2\nu_4) \leftarrow 2\nu_4$  transition (middle signal), and a  $(\nu_3 + \nu_4) \leftarrow \nu_4$  dyad-octad transition (bottom signal). All these signals are given on a same time scale.

that the populations in the dyad states of the A symmetry species are still increasing, reaching a maximum after about 10  $\mu\text{s}$  at these pressures.

To obtain a more quantitative understanding of the various processes involved in the relaxation, the DR signals obtained with the available probes have been studied in detail at different time scales.

(a) *Tetradecad States Probing.* As shown above, the rising (or decaying) part of the DR signals, obtained by probing  $3\nu_3 \leftarrow 2\nu_3(\text{F}_2)$  (or  $2\nu_3(\text{F}_2) \leftarrow \nu_3$ ) transitions in which the lower (or upper) level is directly laser-excited, can be fitted by two exponential functions: the fastest and strongest one is due to the rotational relaxation; the slowest one can be attributed to intermode energy transfer processes that lead to energy redistribution among the vibrational states of the tetradecad. The determination of the rate corresponding to this second exponential function is relatively imprecise since its contribution to the signal is rather small. It is better to probe  $3\nu_3 \leftarrow 2\nu_3(\text{F}_2)$  transitions where the lower rotational level is not the laser-excited level. These signals exhibit first a very fast initial decrease, due to rotational energy transfer, then a rise, which can be well fitted by two exponential functions of time, the fastest one corresponding to the slowest function discussed when fitting the DR signals considered above like those of Figure 2.

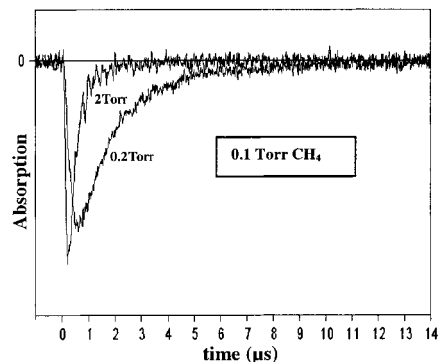


**Figure 7.** DR signals showing the time evolution in population of a rotational level different from the laser-excited level. They are obtained by pumping the  $2\nu_3(\text{F}_2)$   $J = 4$ ,  $A_2$ , 43 level via the  $Q_4$  line and probing a  $3\nu_3 \leftarrow 2\nu_3(\text{F}_2)$   $J = 2$ ,  $A_1$ , 29 transition at  $2970.93 \text{ cm}^{-1}$  in  $\text{CH}_4 + \text{N}_2$  mixtures with 0.1 and 1.9 Torr nitrogen pressure, respectively, the methane pressure being 0.1 Torr for both mixtures.

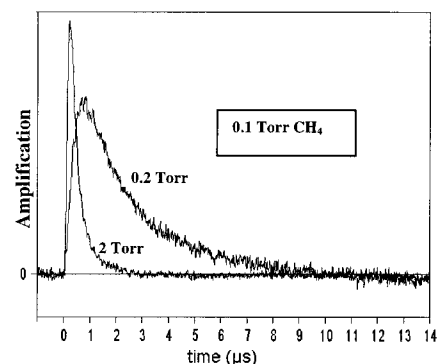


**Figure 8.** DR signals obtained by pumping the  $2\nu_3(\text{F}_2)$ ,  $J = 4$ ,  $A_2$ , 43 level and probing the  $2\nu_3(\text{F}_2)$ ,  $J = 1$ ,  $A_2$ , 18  $\leftarrow \nu_3$ ,  $J = 2$ ,  $A_1$ , 4 transition at  $2963.99 \text{ cm}^{-1}$ , with the same  $\text{CH}_4 + \text{N}_2$  mixtures as in Figure 7.

Two typical DR signals obtained by pumping via  $Q_4$  and probing a  $3\nu_3 \leftarrow 2\nu_3(\text{F}_2)$   $J = 2$ ,  $A_1$  transition at  $2970.93 \text{ cm}^{-1}$  are given in Figure 7. For both signals, the methane pressure is 0.1 Torr, and the nitrogen pressure is 0.1 Torr in one case and 1.9 Torr in the other one. Obviously, the nitrogen molecules are efficient collision partners for depleting the  $2\nu_3(\text{F}_2)$  vibrational state.

The same effect can be observed by probing  $2\nu_3(\text{F}_2)$ ,  $J \leftarrow \nu_3$  transitions with  $J$  different from the pumped level. The increase of the relaxation rate due to the addition of nitrogen to a given methane pressure is obvious in Figure 8 giving two DR signals obtained with the same pressures as for the signals given in Figure 7, by pumping to the  $2\nu_3(\text{F}_2)$ ,  $J = 4$ ,  $A_2$  level and probing the  $2\nu_3(\text{F}_2)$ ,  $J = 1$ ,  $A_2$ , 18  $\leftarrow \nu_3$ ,  $J = 2$ ,  $A_1$ , 4 transition at  $2963.99 \text{ cm}^{-1}$ . Such DR signals have been recorded at methane pressures ranging from 0.025 to 0.6 Torr and methane molar fractions down to 1%.

Two relaxation rates are deduced from exponential fits of all these signals. Plots of these rates versus nitrogen pressure are given in Figure 9 for mixtures with 100 mTorr partial methane pressure. The rate constants corresponding to  $\text{CH}_4\text{-N}_2$  collisions deduced from the slopes of such plots are found to be equal to  $(2 \pm 0.6)$  and  $(0.4 \pm 0.1) \mu\text{s}^{-1} \text{ Torr}^{-1}$ , respectively.

(b) *Pentad States Probing.* When the probe frequency is tuned to a  $2\nu_3(\text{F}_2) \leftarrow \nu_3$  transition, the transient population of the  $\nu_3$  pentad states can be investigated by considering the absorbed part of DR signals such as that given in Figure 10. Of course, the time evolution depends on the populations of both the tetradecad state and the pentad state, and thus it is not possible to deduce directly from such signals the rate constant for the filling of the  $\nu_3$  state. However, it is clear that the probe beam

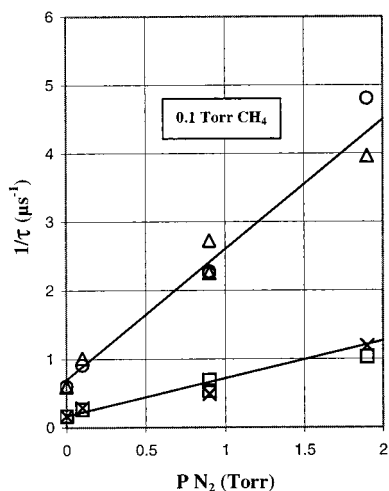


**Figure 9.** Variation, versus nitrogen pressure, of the two rates of depletion of the  $2\nu_3$  ( $F_2$ ) state deduced from exponential fits of DR signals obtained by pumping the  $2\nu_3(F_2)$ ,  $J = 4$ ,  $A_2$ , 43 level and probing the  $3\nu_3 \leftarrow 2\nu_3(F_2)$ ,  $J = 2$ ,  $A_1$ , 29 transition ( $\Delta$  and  $\times$ ) and the  $2\nu_3$  ( $F_2$ ),  $J = 1$ ,  $A_2$ , 18  $\leftarrow \nu_3$ ,  $J = 2$ ,  $A_1$ , 4 transition ( $\circ$  and  $\square$ ), in  $\text{CH}_4 + \text{N}_2$  mixtures with 0.1 Torr methane pressure. The rate constants corresponding to  $\text{CH}_4\text{-N}_2$  collisions, deduced from the slopes of the linear regressions, are found to be equal to  $(2 \pm 0.6)$  and  $(0.4 \pm 0.1) \mu\text{s}^{-1} \text{Torr}^{-1}$ , respectively.

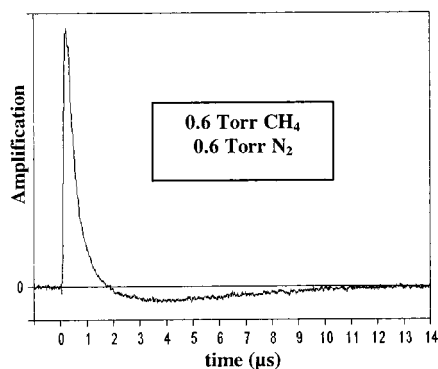


**Figure 10.** DR signal obtained by pumping the  $2\nu_3(F_2)$ ,  $J = 4$ ,  $A_2$ , 43 level and probing the  $2\nu_3(F_2)$ ,  $J = 1$ ,  $A_2$ , 18  $\leftarrow \nu_3$ ,  $J = 2$ ,  $A_1$ , 4 transition, in  $\text{CH}_4 + \text{N}_2$  mixtures with 0.6 Torr methane pressure and 0.6 Torr nitrogen pressure. The absorbed part of the signal is representative of the time evolution of the  $\nu_3$  state population.

becomes absorbed earlier when the  $2\nu_3(F_2)$  depletion becomes faster upon the effect of collisions with nitrogen molecules, which is observed by comparing the DR signals obtained with 0.6 and 34 Torr  $\text{N}_2$  pressure in Figure 10 and Figure 6, respectively. But it can be seen that the time to reach maximum absorption of the probe beam, that is the time to reach maximum population in  $\nu_3$  levels, depends very little on the  $\text{N}_2$  partial pressure as long as the methane molar fraction is lower than 50%.

When the probe frequency is tuned to a  $(\nu_3 + 2\nu_4) \leftarrow 2\nu_4$  transition, the transient population of the  $2\nu_4$  pentad states is well observed in the absorbed portion of DR signals such as that of Figure 11 obtained with a mixture containing 0.6 Torr  $\text{CH}_4$  and 11.4 Torr  $\text{N}_2$ . In this 5% mixture, the maximum population in the  $2\nu_4$  state is reached 4  $\mu\text{s}$  after laser excitation, which is the same delay as for the 1.75% mixture of Figure 6.

Actually, in  $\text{CH}_4\text{-N}_2$  mixtures with a methane molar fraction in the 10 to 1% range, the time to reach maximum population in all pentad levels was found to be quasi independent of the nitrogen pressure and inversely proportional to the methane pressure. In this range, as can be seen in Figure 12, for 1 Torr

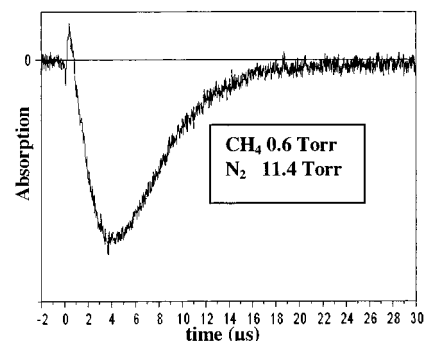


**Figure 11.** DR signal obtained by pumping the  $2\nu_3(F_2)$ ,  $J = 4$ ,  $A_2$ , 43 level and probing a  $(\nu_3 + 2\nu_4) \leftarrow 2\nu_4$  transition, at  $2970.50 \text{ cm}^{-1}$ , in  $\text{CH}_4 + \text{N}_2$  mixtures with 0.6 Torr methane pressure and 11.4 Torr nitrogen pressure. The absorbed part of the signal is representative of the time evolution of the  $2\nu_4$  state population.

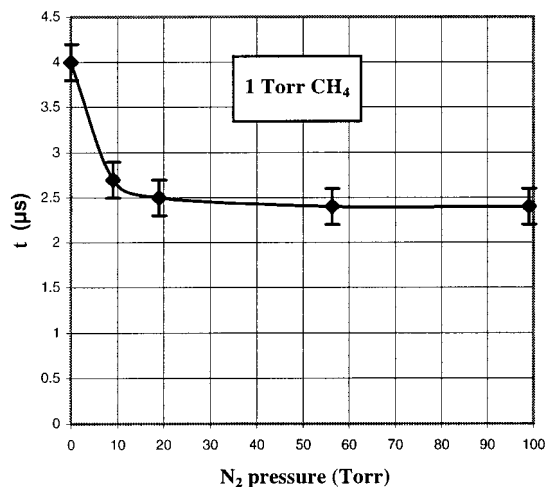


**Figure 12.** Plot, versus nitrogen pressure, of the delay time to reach maximum transient population in pentad levels for 1 Torr  $\text{CH}_4$  pressure.

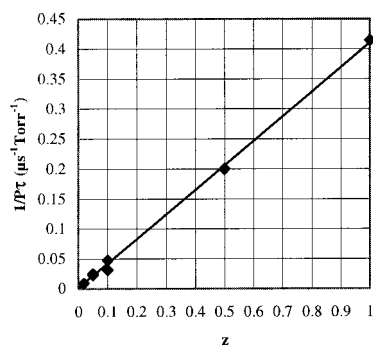


**Figure 13.** Plot of the measured rate constant for the depletion of the  $2\nu_4$  state versus the molar fraction  $z$  of methane in  $\text{CH}_4 + \text{N}_2$  mixtures, showing that this relaxation is independent of the nitrogen pressure.

$\text{CH}_4$  pressure, the time delay to reach maximum population is equal to 2.4  $\mu\text{s}$ .

As the molecules in the  $2\nu_4$  state are quenched, the DR signal rises. This rise is well fitted by an exponential function of time, the rate of which is proportional to the methane pressure with a rate constant equal to  $(0.4 \pm 0.04) \mu\text{s}^{-1} \text{Torr}^{-1}$ , as shown in Figure 13.

These results clearly show that the main processes involved in the increase and decrease of the population in the pentad states are near-resonant V-V energy transfer processes implying only  $\text{CH}_4\text{-CH}_4$  collisions as it has been assumed.

(c) *Dyad States Probing.* The time evolution of the transient populations in the states of the dyad has been investigated by

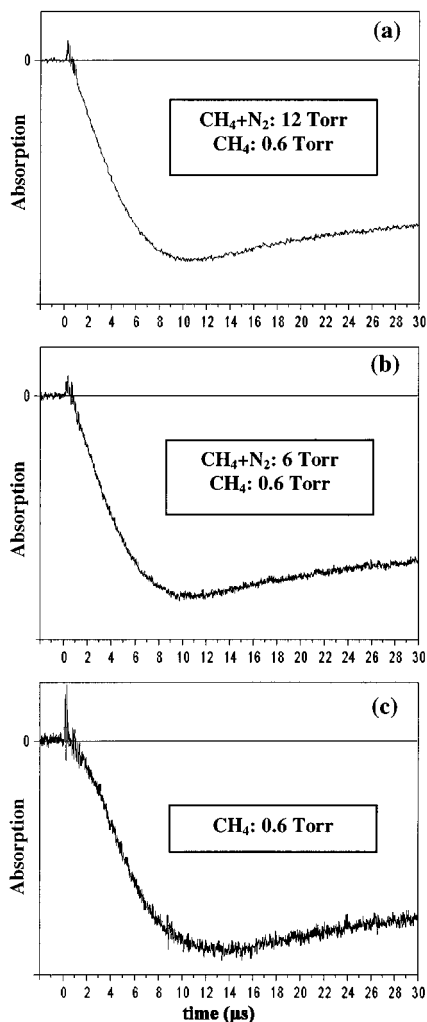


**Figure 14.** DR signals obtained by pumping the  $2\nu_3(F_2)$ ,  $J = 1$ ,  $A_2$ , 18 level via the  $R_0$  line and probing a  $(\nu_3 + \nu_4) \leftarrow \nu_4$  transition of same A symmetry species, in  $\text{CH}_4\text{-N}_2$  mixtures with  $\text{CH}_4$  molar fractions  $z = 0.05$  and  $0.1$  for signals a and b, respectively, and in neat methane for signal c, the methane pressure being  $0.6$  Torr in the three cases.

probing dyad–octad transitions. Such typical DR signals are given in Figure 14. As it will be discussed, they do not present significant amplification of the probe beam because deactivation of the tetradecad to the octad is coupled to promotion into the dyad. Thus, the increase in population of the octad level (upper level of the probed transition) could not be investigated. These signals show a decay mainly due to an increase of population in the states of the dyad, followed by a slower increase toward thermodynamic equilibrium. They are all obtained by pumping with  $R_0$  the  $2\nu_3(F_2)$ ,  $J = 1$ ,  $A_2$  level and probing a  $(\nu_3 + \nu_4) \leftarrow \nu_4$  transition of same symmetry species at  $2949.81\text{ cm}^{-1}$ , in  $\text{CH}_4\text{-N}_2$  mixtures with  $\text{CH}_4$  molar fractions equal to 5 and 10%, respectively, for the signals of Figure 14a,b, and in neat methane for the signal of Figure 14c, the methane pressure being in all cases  $0.6$  Torr.

All these signals have almost the same behavior, showing that processes implying only  $\text{CH}_4\text{-CH}_4$  collisions (i.e., near-resonant V–V transfer) are also predominant in the increase of population in the  $\nu_4$  state. Indeed, the signals in Figure 14a,b, obtained for two different mixtures with the same  $\text{CH}_4$  pressure, can be superimposed and more generally all the signals obtained with  $\text{CH}_4$  molar fraction ranging from 1 to 10% have the same behavior. However, as the nitrogen molar fraction decreases,

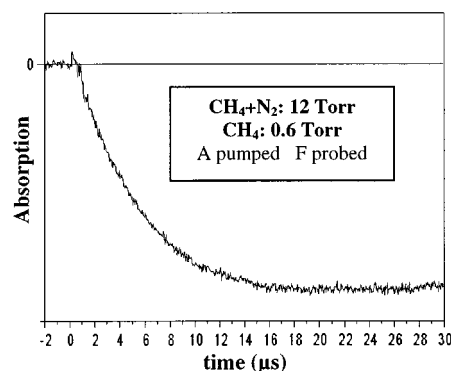


**Figure 15.** DR signals obtained by probing a transition of a symmetry type different from that of the laser-excited level. It has been observed by pumping a level of symmetry A via the  $R_0$  line and by probing a transition of F symmetry in a same mixture as in Figure 14a.

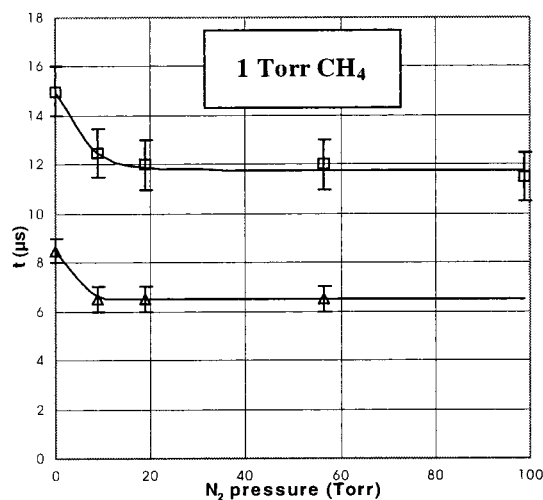


**Figure 16.** Plot, versus nitrogen pressure, of the time to reach maximum transient population in dyad states of the same symmetry as that of the pumped level ( $\Delta$ ) and of different symmetry ( $\square$ ), for a methane pressure of  $1$  Torr.

the initial part of the DR signal is slowed as seen on the signal of Figure 14c obtained in neat methane.

The DR signals of Figure 14, obtained by probing a transition of the same A symmetry type as that of the laser excited level in the tetradecad, exhibit, after the maximum of absorption, a time rise much faster than the rise back to thermodynamic equilibrium due to the V-T/R de-excitation of the dyad. This time rise reveals a decrease in the population of levels of A symmetry, while the DR signals obtained by probing a transition of a symmetry type different from that of the laser-excited level do not exhibit this feature as illustrated by the DR signal given in Figure 15. It is obtained by pumping with  $R_0$  a level of A symmetry in a mixture of  $0.6$  Torr of methane and  $11.4$  Torr of nitrogen, and by probing a transition of F symmetry at  $2949.526\text{ cm}^{-1}$ . The same result is obtained by probing a transition of E symmetry. Obviously, the time to reach maximum population in dyad levels belonging to symmetry species different from that of the excited molecules is longer showing that, while the population corresponding to A species decreases, those corresponding to E and F species are still increasing. The time to reach maximum population as a function of nitrogen pressure is given in Figure 16 for dyad levels of the same symmetry as the pumped level or of different symmetry species. The time evolution of the signals obtained by probing a transition of a symmetry type different from that of the laser-excited level can

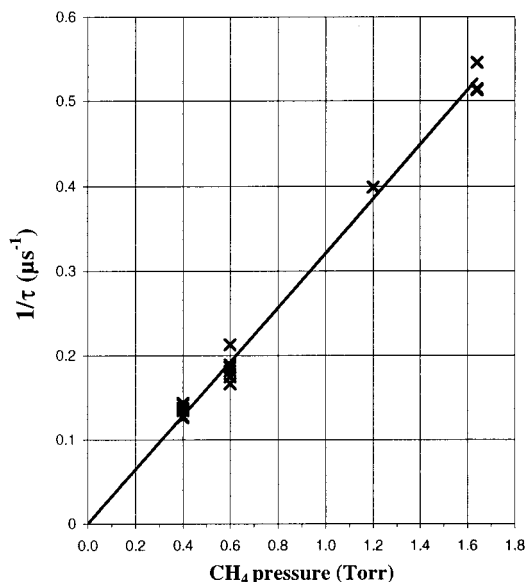


**Figure 17.** Variation, versus the methane pressure, of the decay rate of DR signals obtained by probing dyad–octad transitions in  $\text{CH}_4\text{--N}_2$  mixtures with  $\text{CH}_4$  molar fractions between 1 and 10%.

be well reproduced by a difference of two exponential functions. The decay rate  $1/\tau$ , determined from the first exponential, is found not to depend on the nitrogen pressure for methane molar fraction in the 1–10% range. It varies linearly versus the methane pressure as shown in Figure 17. The rate constant relative to the methane pressure is equal to  $0.32 \mu\text{s}^{-1} \text{Torr}^{-1}$ . It is worth mentioning that if several symmetry species are pumped at the same time the apparent decay rates are larger.

Finally, these signals show, after the maximum of absorption, a very slow rise back to equilibrium with the V-T/R rate constant in agreement with the results given by Perrin and Jolicard<sup>5,6</sup> or by Avramides and Hunter<sup>7</sup> (about  $860 \text{ s}^{-1} \text{Torr}^{-1}$  for  $\text{CH}_4\text{--CH}_4$  collisions) and by Siddles et al.<sup>8</sup> or Yardley et al.<sup>9</sup> (about  $700 \text{ s}^{-1} \text{Torr}^{-1}$  for  $\text{CH}_4\text{--CH}_4$  collisions and  $70 \text{ s}^{-1} \text{Torr}^{-1}$  for  $\text{CH}_4\text{--N}_2$  collisions).

## Discussion

As already observed in neat methane,<sup>2</sup> after the excitation of  $\text{CH}_4$  molecules in a selected rotational level of the  $2\nu_3(\text{F}_2)$  state, a fast equilibration of population occurs first in this state among the rotational levels of the same symmetry type as that of the laser-excited one, i.e., of the same nuclear spin modification. Our experimental results show that nitrogen is a very efficient collision partner for depopulation of the rotational levels of methane in the excited vibrational state. The total depopulation rates by  $\text{CH}_4\text{--N}_2$  collisions is found to be independent of  $J$  for the monitored levels ( $J = 1$  to  $J = 4$ ) in the limits of our experimental accuracy. The linear best fit of the total depopulation rate constants versus methane molar fraction leads to  $13 \mu\text{s}^{-1} \text{Torr}^{-1}$  for  $\text{CH}_4\text{--N}_2$  collisions and to  $20.8 \mu\text{s}^{-1} \text{Torr}^{-1}$  for self-collision in agreement with the results of our previous measurements<sup>2</sup> in neat  $\text{CH}_4$ .

Despite the difficulty to measure accurately the state-to-state rotational energy transfers, our results show that the corresponding rate constants are certainly very large. We have observed that, after excitation in a rotational  $J$  level of the  $2\nu_3(\text{F}_2)$  state, levels with rotational quantum number  $J \pm \Delta J$  are very rapidly populated even for  $\Delta J \geq 2$ . For example, the increase in population of the  $J = 2, A_1, 29$  and  $J = 1, A_2, 18$  levels after excitation into the  $J = 4, A_2, 43$  level occurs at

rates of about 3.5 and  $3 \mu\text{s}^{-1}$  for a 0.2 Torr mixture with 50% methane molar fraction as measured from DR signals given in Figures 7 and 8, respectively. These values are very large as compared to the rate coefficient of  $1 \mu\text{s}^{-1} \text{Torr}^{-1}$  determined for octad levels in neat methane.<sup>10</sup>

Following the rotational relaxation, the energy transfer processes involved in the vibrational relaxation of methane from the tetradecad states are essentially intermode transfer and near-resonant V–V energy transfer processes. The intermode transfer processes are known to be very fast between strongly coupled states<sup>10–13</sup> as is the case for the polyads of  $\text{CH}_4$ . They occur not only upon  $\text{CH}_4\text{--CH}_4$  collisions but also with other collision partners as  $\text{N}_2$ . Indeed, our experimental data shows that the addition of nitrogen to methane has for the main effect to accelerate the equilibration of the population within each polyad of interacting states. That first results in a fast decrease in the population of the  $2\nu_3(\text{F}_2)$  excited state, which is well observed by probing  $3\nu_3 \leftarrow 2\nu_3(\text{F}_2)$  as well as  $2\nu_3(\text{F}_2) \leftarrow \nu_3$  transitions. The rate constants deduced from these measurements may be due to different types of intermode transfer: transfer between stretching modes  $\nu_1 \leftrightarrow \nu_3$ , transfer between stretching and bending modes  $\nu_s \leftrightarrow 2\nu_b$  and transfer between bending modes  $\nu_2 \leftrightarrow \nu_4$ . Intermode transfers between Coriolis coupled stretching states  $2\nu_3 \leftrightarrow (\nu_1 + \nu_3) \leftrightarrow 2\nu_1$  are probably the fastest ones contributing to the redistribution of excited molecules among the states of the tetradecad. However, a large coupling is known<sup>14</sup> to exist in the tetradecad between  $2\nu_3$  and  $(\nu_3 + \nu_2 + \nu_4)$  and more generally between  $2\nu_s$  stretching and  $(\nu_s + 2\nu_b)$  combination states. Let us recall that the fast increase of population in  $(\nu_3 + 2\nu_4)$  has been observed by probing a  $(\nu_3 + 2\nu_4) \leftarrow 2\nu_4$  transition even though the initial amplification is too weak to deduce a rate constant for this transfer. Indeed, the redistribution of molecules laser-excited in the  $2\nu_3(\text{F}_2)$  state among all the states of the tetradecad leads to only a very small increase in population of these states, and in particular of the upper level of the probed transition.

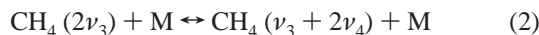
For lack of probe connected to other tetradecad states, it is difficult, in neat methane, to assess the part played by intermode transfer processes filling other tetradecad states and by near-resonant V–V energy transfer processes filling lower polyads in the depopulation of the  $2\nu_3$  levels. As the near resonant V–V energy transfer processes, involving the exchange of one  $\nu_3$  or  $\nu_4$  quantum between two  $\text{CH}_4$  molecules, occur only by collision between methane molecules, it is particularly interesting to study the evolution of the rates as a function of the foreign gas pressure for it allows one to determine the part played by the intermode transfer processes. In previous measurements<sup>2</sup> performed in neat methane, the rate constant corresponding to the second exponential function fitting the depopulation of  $2\nu_3(\text{F}_2)$ , i.e.,  $(1.7 \pm 0.2) \mu\text{s}^{-1} \text{Torr}^{-1}$ , was assumed to be due to the relaxation of the states of the tetradecad by near-resonant V–V energy transfers coupling the tetradecad to the lower polyads. Indeed, as it can be seen in Figures 6 and 10, the last part of the time decrease of DR signals obtained by probing  $2\nu_3(\text{F}_2) \leftarrow \nu_3$  transitions shows an absorption of the probe beam, which means that the lower level of the probed transition, namely a  $\nu_3$  level, is populated. However, as the nitrogen partial pressure is increased, the rate of depopulation of the probed tetradecad levels increases, showing that the measured rate constant corresponds to both intermode and near-resonant V–V energy transfer processes.

The  $\nu_3$  state is populated by different near-resonant V–V energy transfer processes: (i) processes involving exchange of a  $\nu_3$  quantum between  $\text{CH}_4$  molecules, which result in direct

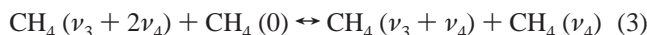
population of the  $\nu_3$  state:



(ii) processes involving exchanges of  $\nu_4$  quanta that require a first phase of equilibration in the tetradecad to populate the combination states that may be illustrated by the following sequences:



and two successive  $\nu_4$  quantum exchanges:



As in the tetradecad, a fast equilibration of population due to intermode transfer processes occurs among the states of each polyad upon collisions with  $\text{CH}_4$  and with  $\text{N}_2$ . This means that the  $\nu_4$  quantum exchanges may occur via another phase of intermode transfer populating the bending states



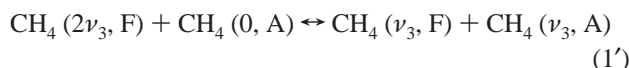
followed by  $\nu_4$  quantum exchanges and intermode equilibration in the pentad states



and also via equilibration in the octad states:



The processes involving exchange of a  $\nu_3$  quantum between  $\text{CH}_4$  molecules have been neglected in previous studies<sup>10</sup> on  $\text{CH}_4$  relaxation. But if the pentad states were filled only via  $\nu_4$  quantum exchange processes only rovibrational levels corresponding to the same symmetry species as the laser-excited one would be populated. In reality, we have observed a weak but fast increase in population of pentad levels corresponding to symmetry species different from the excited one. For instance, by pumping the  $\text{Q}_5$  multiplet of the  $2\nu_3(\text{F}_2) \leftarrow 0$  transition that has no A symmetry component, we have observed an increase of population in  $\nu_3$  levels of A symmetry by probing this symmetry species via selected  $2\nu_3(\text{F}_2) \leftarrow \nu_3$  transitions. This result implies the exchange of a  $\nu_3$  quantum between  $\text{CH}_4$  molecules, as in process (1), because A levels of  $\nu_3$  cannot be populated otherwise than by collisions with  $\text{CH}_4$ , upon which molecules on A symmetry levels of the ground state are promoted into the  $\nu_3$  state. This is illustrated by specifying in the process (1) the spin modification of the laser-excited level which can be written in case of excitation of the F spin modification:



The existence of different pathways to populate the  $\nu_3$  levels explains why the rate corresponding to the population of the pentad depends also on the nitrogen pressure for mixtures containing large methane molar fraction. Indeed, the  $\text{CH}_4\text{-N}_2$

collisions increase the contribution of the pathway involving both intermode transfer and  $\nu_4$  quantum exchange processes.

The near-resonant V–V energy transfer processes lead to the gathering of excited molecules in the states of the lowest polyad, namely, the  $\nu_2$  and  $\nu_4$  states. So the increase of population in these states is essentially due to these processes and thus depends mainly on  $\text{CH}_4\text{-CH}_4$  collisions.

However, as observed for DR signals obtained in gas mixtures by probing dyad–octad transitions, the  $\text{CH}_4\text{-N}_2$  collisions are not without effect on such signals, as previously seen in Figure 14 for the  $\nu_3 + \nu_4 \leftarrow \nu_4$  transition. For instance, for gas samples with the same partial pressure of methane, the time to reach maximum population in the  $\nu_4$  state is shorter in  $\text{CH}_4\text{-N}_2$  mixtures than in neat methane. This is certainly due to the intermode transfer processes which, upon  $\text{CH}_4\text{-N}_2$  collisions, accelerate the equilibration between stretching and bending modes of each polyad.

The upper level of the dyad–octad probed transitions has no contribution to DR signals. Indeed, the near-resonant V–V energy transfer processes, which give rise to an increase of population in the states of the octad, induce a corresponding increase of population in the states of the dyad. This is illustrated by processes (3) and (6) implying exchange of one  $\nu_4$  quantum: upon such processes, the de-excitation of a molecule from the tetradecad to the octad gives rise to the excitation of another molecule from the fundamental state to a state of the dyad. Then, after different steps of relaxation, the de-excitation of one molecule from the tetradecad leads to the excitation of four molecules in the states of the dyad. In particular, the cascading de-excitation of a  $\text{CH}_4$  molecule from the  $4\nu_4$  state leads successively this molecule to the  $3\nu_4$ ,  $2\nu_4$ , and  $\nu_4$  states, at each step a molecule being excited from the fundamental state to the  $\nu_4$  state. The cascading de-excitation occurs only for levels of the same symmetry as the laser-excited level, while the molecules that are raised into the  $\nu_4$  state from the ground state are of any possible symmetry respecting the distribution of molecules in the different spin modifications (5/16 in A, 9/16 in F, and 2/16 in E). Consequently, when the pump is tuned to an A symmetry transition for instance, the populations of A symmetry levels are in an excess as compared to that of E or F symmetry levels. Then a vibrational swap occurs between molecules of different symmetry types until an equilibrium is achieved. This effect induces a decrease in the population of levels of A symmetry which have been seen on the DR signals of Figure 14 that exhibit first a faster rise due to the vibrational swap followed by a much slower one due to V-T/R de-excitation.

## Conclusions

The collisional relaxation of methane in mixture with nitrogen molecules has been studied using time-resolved IR–IR double-resonance technique. The time behavior of the populations of several levels belonging to various rotational and vibrational states were obtained as a function of the partial pressures of  $\text{CH}_4$  and  $\text{N}_2$ . A better view of the relaxation mechanisms is obtained owing to the numerous transitions found in various vibrational bands and to the observed effect of nitrogen. It has been observed that nitrogen molecules are very efficient to redistribute the rotational energy among the rotational levels of the same symmetry. The energy is then spread out over the tetradecad levels of the same symmetry species as that of the laser-excited one by intermode transfer processes between stretching and bending mode, which occur also upon collisions with  $\text{N}_2$  molecules. The lower polyads are more slowly



populated. In pure methane, the more efficient vibrational deactivation processes are V–V transfers. In methane–nitrogen mixtures, as the partial pressure of nitrogen increases, the populating rate of the lower polyads increases very slowly because the V–T/R processes are much slower. In addition, the excited levels corresponding to a symmetry type (spin modification) different from that of the pumped level are not populated by collision with nitrogen but only by V–V transfer processes that are expected to be more efficient at lower temperature.

Further investigations at lower temperature are underway as well as the development of a detailed kinetic model of the vibrational relaxation after excitation in the tetradecad. The model should be capable of reproducing the observed evolution of populations with different collision partners and at various temperatures.

**Acknowledgment.** The authors are glad to thank Dr. Claude Camy-Peyret, Director of LPMA, for his support in this project and for his careful reading of the manuscript.

### References and Notes

- (1) Doyennette, L.; Menard-Bourcin, F.; Menard, J.; Boursier, C.; Camy-Peyret, C. *J. Phys. Chem. A* **1998**, *102*, 3849.
- (2) Menard-Bourcin, F.; Doyennette, L.; Menard, J.; Boursier, C. *J. Phys. Chem.* **2000**, *10*, 1021.
- (3) Robert, O.; Champion, J.-P. Université de Bourgogne. Dijon, France, private communication.
- (4) The assigned quantum numbers J, C, N represent the angular momentum, the rovibrational symmetry, and a running number according to increasing energies within the polyads, see Champion, J.-P.; Loëte, M.; and Pierre, G. In *Spectroscopy of the Earth's Atmosphere and Interstellar Medium*; Rao, K. N.; Weber, A., Eds.; Academic: Columbus, 1992; pp 339–422; see also Wenger, Ch.; Champion, J.-P., Spherical Top Data Systems (STDS) software for the simulation of spherical top spectra, *JQSRT* **1998**, *59*, 471.
- (5) Perrin, M. Y. *Chem. Phys. Lett.* **1982**, *93*, 515.
- (6) Perrin, M. Y.; Jolicard, G. *Chem. Phys. Lett.* **1986**, *127*, 118.
- (7) Avramides, E.; Hunter, T. F. *Chem. Phys.* **1981**, *57*, 441.
- (8) Siddles, R. M.; Wilson, G. H.; Simpson, C. J. S. M. *Chem. Phys.* **1994**, *188*, 99.
- (9) Yardley, J. T.; Fertig, M. N.; Moore, C. B. *J. Chem. Phys.* **1970**, *52*, 1450.
- (10) Klaassen, J. J.; Coy, S. L.; Steinfeld, J. I.; Abel, B. *J. Chem. Phys.* **1994**, *101*, 10553.
- (11) Menard-Bourcin, F.; Doyennette, L., *J. Chem. Phys.* **1988**, *88*, 5506.
- (12) Doyennette, L.; Menard-Bourcin, F., *J. Chem. Phys.*, **1988**, *89*, 5578.
- (13) Bronnikov, D. K.; Kalinin, D.V.; Rusanov, V. D.; Filimonov, YU. G.; Selivanov, G.; Hilico, J. C. *J. Quant. Spectrosc. Radiat. Transfer*, **1998**, *60*, 1053.
- (14) Georges, R.; Herman, M.; Hilico, J.-C.; Robert, O. *J. Mol. Spectrosc.* **1998**, *187*, 13 and references therein.